

## High-yield synthesis of conductive carbon nanotube tips for multiprobe scanning tunneling microscope

H. Konishi, Y. Murata, W. Wongwiryapan, M. Kishida, K. Tomita, K. Motoyoshi, S. Honda, and M. Katayama<sup>a)</sup>

*Division of Electrical, Electronic and Information Engineering, Graduate School of Engineering, Osaka University, 2-1 Yamadaoka, Suita, Osaka 565-0871, Japan*

S. Yoshimoto, K. Kubo, R. Hobara, I. Matsuda, and S. Hasegawa

*Department of Physics, School of Science, University of Tokyo, 7-3-1 Hongo, Bunkyo-ku, Tokyo 113-0033, Japan*

M. Yoshimura

*Nano High-Tech Research Center, Toyota Technological Institute, 2-12-1 Hisakata, Tempaku-ku, Nagoya 468-8511, Japan*

J.-G. Lee and H. Mori

*Research Center for Ultra-High Voltage Electron Microscopy, Osaka University, 7-1 Mihogaoka, Ibaraki, Osaka 567-0047, Japan*

(Received 16 October 2006; accepted 18 December 2006; published online 25 January 2007)

We have established a fabrication process for conductive carbon nanotube (CNT) tips for multiprobe scanning tunneling microscope (STM) with high yield. This was achieved, first, by attaching a CNT at the apex of a supporting W tip by a dielectrophoresis method, second, by reinforcing the adhesion between the CNT and the W tip by electron beam deposition of hydrocarbon and subsequent heating, and finally by wholly coating it with a thin metal layer by pulsed laser deposition. More than 90% of the CNT tips survived after long-distance transportation in air, indicating the practical durability of the CNT tips. The shape of the CNT tip did not change even after making contact with another metal tip more than 100 times repeatedly, which evidenced its mechanical robustness. We exploited the CNT tips for the electronic transport measurement by a four-terminal method in a multiprobe STM, in which the PtIr-coated CNT portion of the tip exhibited diffusive transport with a low resistivity of  $1.8 \text{ k}\Omega/\mu\text{m}$ . The contact resistance at the junction between the CNT and the supporting W tip was estimated to be less than  $0.7 \text{ k}\Omega$ . We confirmed that the PtIr thin layer remained at the CNT-W junction portion after excess current passed through, although the PtIr layer was peeled off on the CNT to aggregate into particles, which was likely due to electromigration or a thermally activated diffusion process. These results indicate that the CNT tips fabricated by our recipe possess high reliability and reproducibility sufficient for multiprobe STM measurements.

© 2007 American Institute of Physics. [DOI: [10.1063/1.2432253](https://doi.org/10.1063/1.2432253)]

### I. INTRODUCTION

Carbon nanotubes<sup>1</sup> (CNTs) exhibit remarkable structural, mechanical, and chemical properties such as small radius, high aspect ratio, mechanical robustness, flexibility, high electrical conductivity, and chemical inertness.<sup>2</sup> These properties have made CNTs a promising tip material for scanning probe microscopy (SPM) applications<sup>3</sup> such as atomic force microscopy (AFM) and scanning tunneling microscopy (STM). A CNT tip for SPM offers important advantages over conventional metal tips by virtue of high-lateral-resolution imaging, tracing of rough surfaces with steep and deep features, preventing the multitip effect, retention of structural perfection of tip apex, and reducing damage to delicate samples. Moreover, in electronic transport measurement on the nanometer scale using a multiprobe STM,<sup>4–19</sup> the CNT tips are expected to reduce the probe spacing between the

tips and also contact areas on samples compared with electrochemically sharpened metal tips. In the case of its AFM application,<sup>3,20,21</sup> the CNT tip has already proven the above-mentioned advantages. The CNT tip for AFM is well established and is now commercially available. However, when the CNT is applied to a STM tip,<sup>3,22–25</sup> one meets serious roadblocks in facilitating durability, mechanical robustness, and electrical conductivity between a CNT and the supporting metal tip. This is because the junction between the CNT and the supporting tip is rather loose and not always electrically well connected. In this sense, the CNT tip for STM has not yet been established, although, in single-probe operation, it has demonstrated great advantages in the high-resolution imaging and spectroscopy compared with the conventional metal tip.<sup>22–25</sup> To exploit the CNT tips as conductive probes, overcoming above roadblocks and a high-yield synthesis method are highly required. In our previous studies, for single-probe STM, electrical conductivity between a CNT and the supporting metal tip has been improved by wholly

<sup>a)</sup>Electronic mail: katayama@nmc.eei.eng.osaka-u.ac.jp

coating the CNT tip uniformly with a thin metal layer by pulsed laser deposition (PLD).<sup>24–26</sup> However, breakthroughs in the durability and mechanical robustness of the CNT tip remain to be achieved.

The following attachment methods have been adopted so far for CNT tip preparation: (1) attaching a CNT to a metal-tip apex individually in a scanning electron microscope<sup>27,28</sup> (SEM) and depositing amorphous carbon locally by electron beam deposition (EBD) to strengthen adhesion, (2) growing a CNT directly on a metal-tip apex by chemical vapor deposition (CVD),<sup>29</sup> and (3) attaching a CNT to a metal-tip apex by ac dielectrophoresis.<sup>30,31</sup> Attaching a CNT in a SEM chamber by EBD requires great skill and a goniometer stage for aligning and manipulating the CNT, and the throughput is very low. For the direct growth of a CNT by CVD, it is difficult to control the length, density, position, and orientation of the CNT. In contrast, attaching a CNT by ac dielectrophoresis affords high-yield synthesis of the CNT tip without complicated manipulators and skill. However, the junction between the CNT and the supporting metal tip is not stiff enough, which causes serious problems on the practical durability of the tip such as vanishing of the CNT from the tip apex during tip transportation. In multiprobe STM, this problem is especially more serious than in single-probe STM, since several CNT tips must be installed into a chamber at once and must have direct contact with measuring objects. To fully develop the CNT tips as conductive probes in multiprobe STM, it is indispensable to satisfy the requirements in practical durability, mechanical robustness, and stable electrical conductivity. However, no breakthrough in overcoming the roadblocks has been reported so far.

In this article, conductive CNT tips for multiprobe STM were successfully synthesized with high yield. We applied dielectrophoresis to attach a CNT on a supporting W tip, and reinforced the adhesion between them by EBD of amorphous hydrocarbon and subsequent heat treatment, and finally coated the tip wholly with a 6-nm-thick PtIr layer. The survival rate of the CNT tips was improved to more than 90% after long-distance transportation in air, indicating the practical durability of the CNT tip. The shape of the CNT tip was maintained even after 100 repeated contacts with another metal tip, which evidenced the mechanical robustness of the CNT tip. We exploited the CNT tips for the electronic transport measurement by a four-terminal method in a multiprobe STM, in which the PtIr-coated CNT portion of the tip exhibited diffusive transport with a low resistivity of 1.8 k $\Omega$ / $\mu$ m. The contact resistance at the junction between the CNT and the supporting W tip was estimated to be stably less than 0.7 k $\Omega$ . Even though the formation of the PtIr grains was confirmed on the CNT portion of the tip, the PtIr thin layer remained at the CNT-W junction portion after excess current passed through, which led to the reduction of the contact resistance.

## II. EXPERIMENTAL METHOD

Figure 2 shows the best fabrication process for the robust and conductive CNT tips in this study. (a) To prepare the CNT suspension, 0.2 mg of multiwalled CNT (MWNT) was

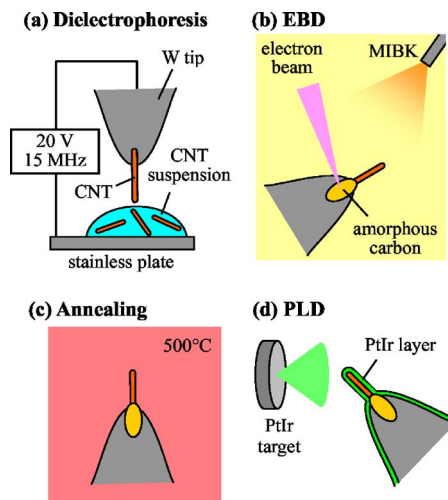


FIG. 1. (Color online) Schematic diagram of the best fabrication process for robust and conductive CNT tips: (a) fabrication of a CNT tip by ac dielectrophoresis, (b) deposition of the amorphous hydrocarbon around the junction portion between the CNT and the W tip by EBD, (c) annealing of the tip at 500 °C, and (d) coating of the tip with a PtIr layer by PLD.

dispersed in 20 ml of dichloroethane, and this solution was sonicated in an ultrasonic bath for 3 h. We used commercially available MWNTs (Materials and Electrochemical Research Corp.) grown by the arc discharge method, which had an average diameter of 20 nm and a length larger than 3  $\mu$ m. (b) A W wire of 0.25 mm in diameter was electropolished with a 2M NaOH solution to prepare a sharpened tip. Then, the CNTs were attached to an apex of a W tip by ac dielectrophoresis in air [Fig. 1(a)].<sup>30</sup> The W tip was dipped into a drop of the CNT suspension on a stainless plate while applying a high-frequency voltage between the tip and the plate. The peak-to-peak ac voltage was 20 V and the frequency was fixed at 15 MHz. It took only a few seconds to attach the CNT onto the end of the W tip. (c) To reinforce the adhesion between the CNT and the W tip, the amorphous hydrocarbon with a thickness of 20 nm was deposited around the junction portion (100  $\times$  300 nm<sup>2</sup>) between the CNT and the W tip by EBD using methyl isobutyl ketone (MIBK) gas with a partial pressure of 1  $\times$  10<sup>-3</sup> Pa in a SEM chamber [Fig. 1(b)]. The electron beam had an energy of 10 keV, a beam spot size of 5 nm, and a current density of 1  $\times$  10<sup>-4</sup> A/cm<sup>2</sup>. Then, the tip was annealed at 500 °C for 30 min using a ceramic heater in vacuum with a pressure of 1  $\times$  10<sup>-4</sup> Pa [Fig. 1(c)]. (d) The reinforced CNT tip was uniformly coated with a 6-nm-thick PtIr thin layer by PLD [Fig. 1(d)]. The coating was carried out at room temperature using a PtIr target (compositional ratio, 80:20 at. %; purity, 99.9%) under a pressure of 1  $\times$  10<sup>-4</sup> Pa. The details of the PLD apparatus were described in our previous papers.<sup>24,32</sup>

To test the durability of the CNT tips, we transported both the CNT tips with and without the reinforcing treatment from Osaka to Tokyo (over 500 km) by train in air. The CNT tips placed on an antistatic mat were packaged in a plastic case, wholly wrapped in cushioning material. The transportation time was 3 h. The average temperature and humidity during the transportation were 20 °C and 50%, respectively. Then, the survival rate and properties of the CNT on the W

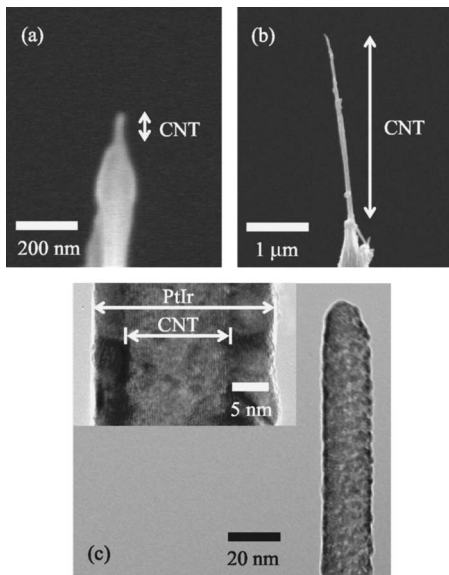


FIG. 2. SEM images of PtIr-coated CNT tips with (a) short and (b) long CNTs, respectively. (c) TEM image of PtIr-coated CNT tip. The inset shows a magnified image of (c).

tip apex were evaluated from the SEM observation. To evaluate the mechanical robustness and electrical conductivity of the tips in multiprobe operation, four CNT tips were installed into an independently driven four-tip STM apparatus with a SEM apparatus.<sup>5,9</sup> All experiments in multiprobe STM were carried out at a pressure of  $1 \times 10^{-6}$  Pa at room temperature under SEM observation. The CNT tip was also introduced into an ultrahigh-vacuum (UHV) single-probe STM system (OMICRON). The clean Si(111)- $7 \times 7$  reconstructed surface was prepared by conventional thermal flashing in UHV. High-resolution transmission electron microscopy (HRTEM) and SEM were utilized to characterize *ex situ* the structural properties of the tips.

### III. RESULTS AND DISCUSSION

Figures 2(a) and 2(b) show typical SEM images of the PtIr-coated CNT tips with relatively short and long CNTs, respectively. The lengths of the CNTs were 100 nm and  $3 \mu\text{m}$ , respectively. The protruding CNTs are straight, and align along the axis direction of the W tip. No CNTs protruding from the side surface of the W tip were found. In Fig. 2(a), the protruding CNT has a diameter of approximately 35 nm. On the other hand, in Fig. 2(b), the root area of the CNTs has a large diameter of 150 nm owing to their bundling. However, the tip apex has a diameter of approximately 30 nm and consists of a single CNT, indicating that the CNTs taper to a sharp point with distance from the root. Figure 2(c) shows a TEM image of a PtIr-coated CNT. The thickness of the PtIr thin layer was estimated to be approximately 6 nm from a magnified image in the inset of Fig. 2(c). Thus, the PtIr coating was successfully achieved with nanometer accuracy reflecting the shape of the MWNT, and the average surface roughness of the layer was less than 0.5 nm. The lattice fringe of graphite can be clearly observed, indicating that the inner MWNT maintained good crystallinity.

TABLE I. Summary of survival rates of CNT tips treated by different processes.

Reinforcing process	No. of samples	No. of surviving tips	Survival rate (%)
Untreated	59	5	8
Annealing $\rightarrow$ EBD	11	5	45
EBD $\rightarrow$ Annealing	16	15	94

To investigate the durability of the CNT tips, we fabricated three types of tips by different procedures: (1)  $500^\circ\text{C}$  annealing in vacuum after the reinforcing by EBD, (2)  $500^\circ\text{C}$  annealing before the EBD, and (3) no annealing nor EBD treatments. After the long-distance transportation in air from Osaka to Tokyo by train, we checked whether the CNTs at the tip apex survived. The survival rates of the CNT tips prepared by the three processes are summarized in Table I. For untreated CNT tips, most tips lost the CNTs at the tip apex. In contrast, the survival rate of the CNT tips was improved markedly by annealing after EBD. Since the amorphous hydrocarbon formed at the CNT-W junction portion by EBD contains hydrogen, it is likely that the improvement in the durability of the CNT tip subjected to vacuum annealing is attributed to the increase in the number of strong carbon-carbon bonds caused by the decrease in the number of weak hydrogen-carbon bonds in amorphous hydrogenated carbon (*a*-C:H). This was supported by previous reports<sup>33,34</sup> that the heating of *a*-C:H film at  $400\text{--}600^\circ\text{C}$  led to hydrogen desorption and caused structural changes.

To evaluate the mechanical robustness of the PtIr-coated CNT tip, the tip was subjected to direct contact with another W tip more than 100 times repeatedly in the multiprobe STM, and the electrical conductivity through the contact point was measured by a two-terminal method at each contact. The inset in Fig. 3 shows a SEM image displaying the contact configuration between two tips. Both tips B and D are PtIr-coated CNT tips. The length and diameter of protruding CNTs of tip B were approximately  $1.2 \mu\text{m}$  and 50 nm, respectively. While the position of tip D was fixed, tip B was moved back and forth with a piezoelectric actuator to make direct contact with and detach from the side surface

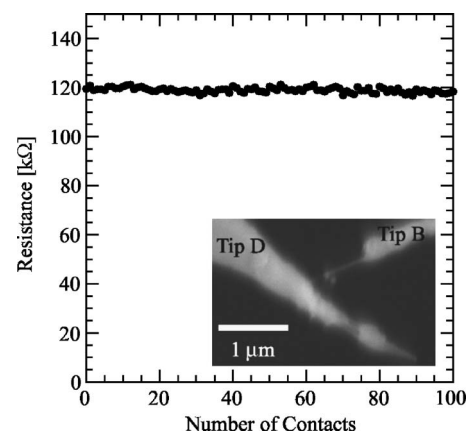


FIG. 3. Two-terminal resistance between tips B and D as a function of number of direct contacts between them. The inset shows a SEM image of the typical contact configuration in multiprobe STM.

of the supporting W tip portion of tip D. The motion of tip B was controlled without a STM feedback system. A bias voltage of 10 mV was applied between tips B and D, monitoring the current between them during the movement of tip B. When the current exceeded a threshold value of 1 nA, the movement of the tip was stopped. Upon the direct contact, the current overran the threshold value. Then, the current-voltage ( $I$ - $V$ ) characteristics between the two tips were measured. It showed an Ohmic character in which the current was proportional to the voltage in the range of  $\pm 100$  mV. Figure 3 shows the two-terminal resistance ( $R_{2t}$ ) between tips B and D measured at each contact. According to a previous study,<sup>26</sup>  $R_{2t}$  is dominated by the contact resistance between the CNT apex of tip B and the side surface of tip D. It was found that  $R_{2t}$  was highly stable at approximately 120 k $\Omega$  during 100 repeated contacts. In the case of conventional metal tips, the resistance scattered from contact to contact due to the variation of contact resistance between the tips, which was caused by the tip deformation during the repeated contacts. The high stability of the measured resistance in our experiment implies that both the contact condition and the structural property of the tip apex of coated CNT were stably maintained during the repeated contacts. Indeed, from the SEM observation, we confirmed that the tip shape did not change, without damage such as deformation and shortening, during the above measurement.

We also demonstrated STM imaging of a Si(111)-7 $\times$ 7 surface (not shown). As reported by Treacy *et al.*<sup>35</sup> and Shimizu *et al.*,<sup>22</sup> since the CNT tip with a relatively long CNT is unsuitable for STM observation owing to the thermal vibration, the PtIr-coated CNT tip with a short CNT (diameter: 30 nm, length: 150 nm) was used. The atomic images of both empty and filled states were obtained stably for a period of over 2 h (maximum time we did the experiment) without degradation of resolution. These results clearly evidence that the junction between the CNT and the W tip was mechanically robust and electrically stable.

Next, we estimated the electrical strength of a PtIr-coated CNT attached to tip B in Fig. 3. The  $I$ - $V$  measurement by the two-terminal method revealed that the PtIr-coated CNT could pass a current of approximately 25  $\mu$ A without any apparent damages, which was the upper-limit current that can be measured using our system. This indicates that the PtIr-coated CNT tip has a current-carrying capability sufficient for practical use in nanometer-scale transport measurements.

We evaluated the electrical conductivity of the CNT tip by a four-terminal method in the multiprobe STM. Figure 4(a) shows a typical SEM image of the configuration of four PtIr-coated CNT tips during the measurement. We performed the electrical characterization of tip A, which has a relatively long CNT whose diameter and length were approximately 35 nm and 3.1  $\mu$ m, respectively. Tip D contacted the end of the PtIr-coated CNT of tip A, and tips B and C were made to contact the CNT portion of tip A. The diameters of tips B, C, and D were 30, 36, and 42 nm, and their lengths were 0.6, 0.6, and 2.3  $\mu$ m, respectively. It is noted that the formation of particles was observed on the CNT of tip A, which represented the PtIr aggregation due to involuntary excessive cur-

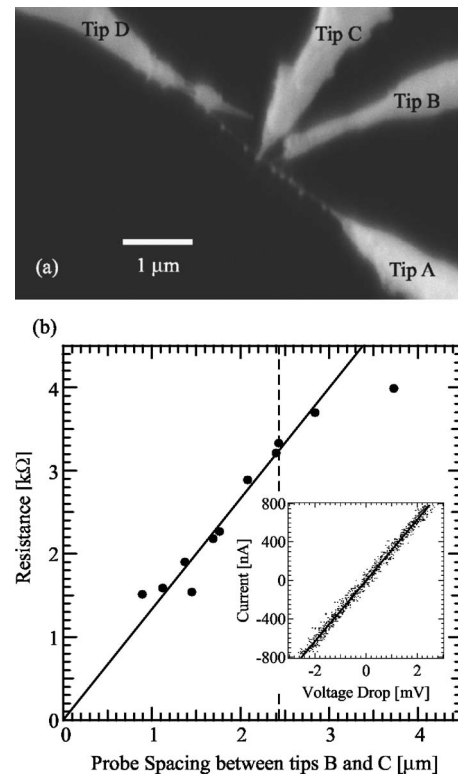


FIG. 4. (a) SEM image of four-terminal configuration of four PtIr-coated CNT tips in multiprobe STM. (b) Dependence of four-terminal resistance on probe spacing between tips B and C ( $L_{BC}$ ). The dashed line indicates the boundary between the CNT and the supporting W tip of tip A. The inset shows current passing through tips A and D vs the voltage drop between tips B and C at  $L_{BC}=1.8$   $\mu$ m.

rent conduction. By measuring the current ( $I_{AD}$ ) passing through from tips A to D, and the voltage drop ( $V_{BC}$ ) between tips B and C, the four-terminal resistance ( $R_{4t} = V_{BC}/I_{AD}$ ) was obtained.  $I_{AD}$  ranged from  $-800$  to  $800$  nA for bias voltages of  $\pm 10$  mV between tips A and D. By shifting the contacting point of tip B on the CNT portion of tip A while fixing the positions of tips A, C, and D,  $R_{4t}$  was measured as a function of the probe spacing ( $L_{BC}$ ) between tips B and C ranging from 0.9 to 3.7  $\mu$ m. Figure 4(b) shows the dependence of  $R_{4t}$  on  $L_{BC}$ . A typical  $I_{AD}$ - $V_{BC}$  curve ( $L_{BC} = 1.8$   $\mu$ m) is shown in the inset, showing linear character.  $R_{4t}$  increased almost linearly with  $L_{BC}$  up to 2.4  $\mu$ m (dashed line), obeying Ohm's law. This result indicates the diffusive transport rather than the ballistic transport of electrons. The resistance ( $R_L$ ) per unit length was estimated to be approximately 1.8 k $\Omega/\mu$ m by piecewise linear fitting. The resistance at  $L_{BC}=3.7$   $\mu$ m was also measured by placing tip B on the supporting W tip portion of tip A, which was the sum of the resistance of the CNT portion itself and the contact resistance ( $R_C$ ) at the junction between the CNT and W tip of tip A. Then,  $R_C$  was estimated to be less than 0.7 k $\Omega$  by subtracting the resistance at  $L_{BC}=2.4$   $\mu$ m (root area of protruding CNT) from that at  $L_{BC}=3.7$   $\mu$ m. In our previous work,<sup>26</sup> the electrical conductivity of the PtIr-coated and bare CNT tips attached on W tips without the heating after EBD was investigated by a three-terminal measurement and a series of two-terminal measurements. The results exhibited that the coating of the PtIr layer stably reduced  $R_C$  to less than

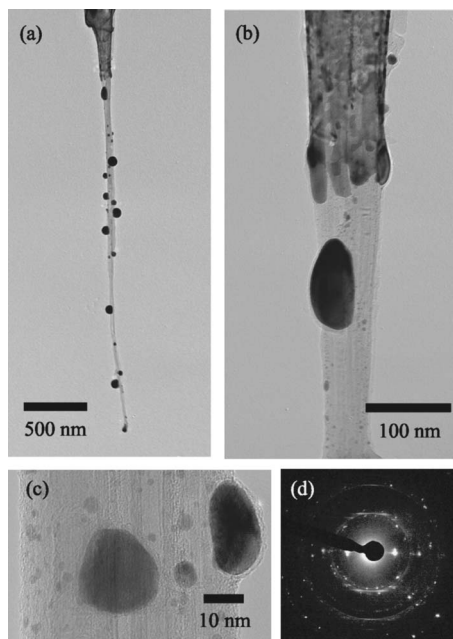


FIG. 5. (a) TEM image of PtIr-coated CNT tip (tip A) after the four-terminal measurement and (b) magnified image of adhesion area. (c) High-resolution TEM image and (d) selected-area electron diffraction pattern of exposed CNT area in (a).

10 k $\Omega$ , which was deduced from the minimum resistance in repeated measurements. In this study, the measured  $R_C$  of less than 0.7 k $\Omega$  was smaller than that in our previous work. This is attributed to the improvement of the adhesion between the CNT and W tip. Thus, we clearly evidenced the usefulness of the combination of the adhesion reinforcement and the PtIr coating in reduction of the resistance  $R_C$  at the CNT-W junction.

The above results can be discussed from the viewpoint of electron transport in suspended MWNT. The conduction mechanism of the MWNT in our experiment is characterized by the following findings. First, it is likely that the measured resistance was not affected by the PtIr coating nor the bundle formation in tip A, but originated from a single MWNT. Since the PtIr layer on the MWNT surface formed the particles as shown in Fig. 5 by the involuntary excess current conduction, tips B and C made direct contact not with the PtIr layer but with the MWNT surface. Also, if tips B and C made contact with different MWNTs in the bundle, respectively,  $R_L$  would exhibit a larger value than that of a single MWNT due to a contact resistance between different MWNTs. Second, the MWNT exhibited diffusive transport as shown in Fig. 4(b) (at least for longer than about 1  $\mu\text{m}$ ). Third, outermost-shell transport in the MWNT may occur under our experimental conditions, since tips B–D were softly placed in contact with the surface of the MWNT only, and the voltage drop was measured in the low-bias regime of  $\pm 10$  mV. It is noted that the measured  $R_L$  of 1.8 k $\Omega/\mu\text{m}$  was an order of magnitude smaller than those of MWNTs in previous studies,<sup>36,37</sup> conducted by a four-terminal method in which CNTs were laid on a substrate. Moreover, our  $R_L$  is comparable to that in the multishell transport of a MWNT with an “entire contact” with the electrodes,<sup>38</sup> although our contacts are with the outermost shell only. Therefore, the

following factors are considered to contribute to our low  $R_L$ . In our experiment, the MWNT was passivated by the PtIr layer until the tip was installed in the multiprobe STM chamber. Moreover, the measurement was carried out in vacuum, and the CNT under measurement was not dispersed on a substrate but was suspended between the electrode tips, so that the MWNT is less affected by external disturbances such as interaction with adsorbed contaminant molecules and the substrate.<sup>39</sup> Consequently, we conjecture that the measured low  $R_L$  represents an intrinsic resistivity in the clean outer shell of the MWNT. This is consistent with the previous report by Bourlon *et al.*:<sup>37</sup> They estimated the  $R_L$  values of the outermost shell and inner shell to be approximately 20 and 1 k $\Omega/\mu\text{m}$ , respectively. This implies that the resistivity measured in our study is as low as that of their inner shell, which is protected by the outer shell.

The structural property of the tip was characterized by TEM after the four-terminal measurement. Figure 5(a) shows a TEM image of tip A after the measurement. The PtIr layer on the CNT aggregated and the inner CNT was exposed. Figure 5(b) shows a magnified image near the CNT-W junction portion in Fig. 5(a). The PtIr layer remained at this portion, indicating that the PtIr layer actually contributed to the reduction of  $R_C$ . Figures 5(c) and 5(d) show a magnified image and a diffraction pattern of the exposed CNT area in Fig. 5(a), respectively. The fringes and (0002) spots of graphite layers were clearly observed, indicating that the crystallinity of the inner shells of CNT was maintained owing to its high current-carrying capacity.<sup>40</sup> The formation of the PtIr particles is likely to be due to electromigration or thermally activated diffusion.<sup>41</sup> The PtIr particle formation did not occur by  $I_{AD}$  ( $< 1 \mu\text{A}$ ) in the four-terminal measurement [the inset of Fig. 4(b)], but resulted from accidental pulsed current of approximately 100  $\mu\text{A}$  upon switching in electrical circuits.

Our results proved the improvement of adhesion between the CNT and the supporting W tip, which can facilitate overcoming the roadblocks in practical durability, mechanical robustness, and electrical conductivity for multiprobe STM application. In the four-terminal measurement, the minimum probe spacing between tips B and C was approximately 0.9  $\mu\text{m}$ . This restriction came from the fact that the CNTs at the apexes of tips B and C were short and therefore the supporting tip portions contact each other as shown in Fig. 4(a). In a previous study,<sup>25</sup> we demonstrated the operation of two CNT tips with a 1- $\mu\text{m}$ -long CNT and achieved a minimum probe spacing of approximately 50 nm. The tips with a CNT of well-controlled length are indispensable for reducing the intertip spacing and adjusting the resistance of the CNT tip itself in multiprobe STM measurements. For this purpose, the cutting of a long CNT is a promising method.<sup>42–45</sup> Using four tips with a length-adjusted CNT and/or sharper supporting metal tips, it is possible to reduce the intertip spacing to approximately 30 nm. Thus, the CNT tips fabricated by our proposed technique offer the potentiality of multiprobe STM for practical use in electrical measurement on the nanometer scale.

## ACKNOWLEDGMENTS

This work was partly supported by the SENTAN Program of the Japan Science and Technology Agency and by a Grant-in-Aid for Scientific Research from the Japan Society for the Promotion of Science. One of the authors (W.W.) acknowledges support from the Japan Society for the Promotion of Science.

- <sup>1</sup>S. Iijima, *Nature* (London) **354**, 56 (1991).
- <sup>2</sup>M. S. Dresselhaus, G. Dresselhaus, and Ph. Avouris, *Carbon Nanotubes; Synthesis, Structure, Properties, and Application* (Springer, New York, 2001).
- <sup>3</sup>H. Dai, J. H. Hafner, A. G. Rinzler, D. T. Colbert, and R. E. Smalley, *Nature* (London) **384**, 147 (1996).
- <sup>4</sup>M. Aono, C.-S. Jiang, T. Nakayama, T. Okuda, S. Qiao, M. Sakurai, C. Thirstrup, and Z.-H. Wu, *Oyo Butsurei* **67**, 1361 (1998) (in Japanese).
- <sup>5</sup>I. Shiraki, F. Tanabe, R. Hobara, T. Nagao, and S. Hasegawa, *Surf. Sci.* **493**, 633 (2001).
- <sup>6</sup>H. Watanabe, C. Manabe, T. Shigematsu, and M. Shimizu, *Appl. Phys. Lett.* **78**, 2928 (2001).
- <sup>7</sup>H. Okamoto, and D. Chen, *Rev. Sci. Instrum.* **72**, 4398 (2001).
- <sup>8</sup>H. Grube, B. C. Harrison, J. Jia, and J. J. Boland, *Rev. Sci. Instrum.* **72**, 4388 (2001).
- <sup>9</sup>S. Hasegawa, I. Shiraki, F. Tanabe, and R. Hobara, *Curr. Appl. Phys.* **2**, 465 (2002).
- <sup>10</sup>J. Onoe, T. Nakayama, M. Aono, and T. Hara, *Appl. Phys. Lett.* **82**, 595 (2003).
- <sup>11</sup>T. Kanagawa, R. Hobara, I. Matsuda, T. Tanikawa, A. Natori, and S. Hasegawa, *Phys. Rev. Lett.* **91**, 36805 (2003).
- <sup>12</sup>K. Takami, J. Mizuno, M. Akai-kasaya, A. Saito, M. Aono, and Y. Kuwahara, *J. Phys. Chem. B* **108**, 16353 (2004).
- <sup>13</sup>K. Takami, M. Akai-kasaya, A. Saito, M. Aono, and Y. Kuwahara, *Jpn. J. Appl. Phys., Part 2* **44**, L120 (2005).
- <sup>14</sup>M. Ishikawa, M. Yoshimura, and K. Ueda, *Jpn. J. Appl. Phys., Part 1* **44**, 1502 (2005).
- <sup>15</sup>O. Guise, H. Marbach, J. T. Yates, Jr., M.-C. Jung, J. Levy, and J. Ahner, *Rev. Sci. Instrum.* **76**, 45107 (2005).
- <sup>16</sup>H. Okino, I. Matsuda, R. Hobara, Y. Hosomura, S. Hasegawa, and P. A. Bennett, *Appl. Phys. Lett.* **86**, 233108 (2005).
- <sup>17</sup>O. Kubo, Y. Shingaya, M. Nakaya, M. Aono, and T. Nakayama, *Appl. Phys. Lett.* **88**, 254101 (2006).
- <sup>18</sup>X. Lin, X. B. He, T. Z. Yang, W. Guo, D. X. Shi, H.-J. Gao, D. D. Ma, S. T. Lee, F. Liu, and X. C. Xie, *Appl. Phys. Lett.* **89**, 43103 (2006).
- <sup>19</sup>P. Jaschinsky, P. Coenen, G. Pirug, and B. Voigtlander, *Rev. Sci. Instrum.* **77**, 93701 (2006).
- <sup>20</sup>S. S. Wong, A. T. Woolley, T. W. Odom, J.-L. Huang, P. Kim, D. V. Zevenov, and C. M. Lieber, *Appl. Phys. Lett.* **73**, 3465 (1998).
- <sup>21</sup>J. H. Hafner, C. L. Cheung, and C. M. Lieber, *Nature* (London) **398**, 761 (1999).
- <sup>22</sup>T. Shimizu, H. Tokumoto, S. Akita, and Y. Nakayama, *Surf. Sci.* **486**, L455 (2001).
- <sup>23</sup>W. Mizutani, N. Choi, T. Uchihashi, and H. Tokumoto, *Jpn. J. Appl. Phys., Part 1* **40**, 4328 (2001).
- <sup>24</sup>T. Ikuno *et al.*, *Jpn. J. Appl. Phys., Part 2* **43**, L644 (2004).
- <sup>25</sup>Y. Murata *et al.*, *Jpn. J. Appl. Phys., Part 1* **44**, 5336 (2005).
- <sup>26</sup>S. Yoshimoto *et al.*, *Jpn. J. Appl. Phys., Part 2* **44**, L1563 (2005).
- <sup>27</sup>H. Nishijima, S. Kamo, S. Akita, Y. Nakayama, K. I. Hohmura, S. H. Yoshimura, and K. Takeyasu, *Appl. Phys. Lett.* **74**, 4061 (1999).
- <sup>28</sup>S. Akita, H. Nishijima, Y. Nakayama, F. Tokumasu, and K. Takeyasu, *J. Phys. D* **32**, 1044 (1999).
- <sup>29</sup>M. Yoshimura, S. Jo, and K. Ueda, *Jpn. J. Appl. Phys., Part 1* **42**, 4841 (2003).
- <sup>30</sup>K. Ueda, M. Yoshimura, and T. Nagamura, Japan Patent No. 3,557,589 (28 May 2004).
- <sup>31</sup>J. Tang, B. Gao, H. Geng, O. D. Velev, L.-C. Qin, and O. Zhou, *Adv. Mater. (Weinheim, Ger.)* **15**, 1352 (2003).
- <sup>32</sup>T. Ikuno, M. Katayama, K. Kamada, S. Honda, J.-G. Lee, H. Mori, and K. Oura, *Jpn. J. Appl. Phys., Part 2* **42**, L1356 (2003).
- <sup>33</sup>B. Dischler, A. Bubenzer, and P. Koidl, *Solid State Commun.* **48**, 105 (1983).
- <sup>34</sup>R. O. Dillon, J. A. Woollam, and V. Katkanant, *Phys. Rev. B* **29**, 3482 (1984).
- <sup>35</sup>M. M. J. Treacy, T. W. Ebbesen, and J. M. Gibson, *Nature* (London) **381**, 678 (1996).
- <sup>36</sup>P. G. Collins, M. Hersam, M. Arnold, R. Martel, and Ph. Avouris, *Phys. Rev. Lett.* **86**, 3128 (2001).
- <sup>37</sup>B. Bourlon, C. Miko, L. Forro, D. C. Glattli, and A. Bachtold, *Phys. Rev. Lett.* **93**, 176806 (2004).
- <sup>38</sup>B. Q. Wei, R. Vajtai, and P. M. Ajayan, *Appl. Phys. Lett.* **79**, 1172 (2001).
- <sup>39</sup>J. Cao, Q. Wang, and H. Dai, *Nat. Mater.* **4**, 745 (2005).
- <sup>40</sup>H. Dai, E. W. Wong, and C. M. Lieber, *Science* **272**, 523 (1996).
- <sup>41</sup>B. C. Regan, S. Aloni, R. O. Ritchie, U. Dahmen, and A. Zettl, *Nature* (London) **428**, 924 (2004).
- <sup>42</sup>S. Akita and Y. Nakayama, *Jpn. J. Appl. Phys., Part 1* **41**, 4887 (2002).
- <sup>43</sup>N. de Jonge, Y. Lamy, and M. Kaiser, *Nano Lett.* **3**, 1621 (2003).
- <sup>44</sup>J. Martinez, T. D. Yuzvinsky, A. M. Fennimore, A. Zettl, R. Garcia, and C. Bustamante, *Nanotechnology* **16**, 2493 (2005).
- <sup>45</sup>A. J. Austin, C. V. Nguyen, and Q. Ngo, *J. Appl. Phys.* **99**, 114304 (2006).